Analysis of imaging modalities for classification of tumoral vs. normal tissues using an FD-FLIM based MMF endoscopy probe

Victoria Fay[1,*], *Genrich* Tolstonog[2, 3], *Christian* Simon[2,3], *Demetri* Psaltis[1], and *Christophe* Moser[1,]

[1]Laboratory of Applied Photonics Devices, EDPO EPFL, 1015 Lausanne, Switzerland
[2]Department of Otolaryngology – Head and Neck Surgery, Lausanne University Hospital and University of Lausanne, Lausanne, Switzerland
[3]AGORA Cancer Research Center, Lausanne, Switzerland

Abstract. Current surgical resections for Head and Neck Cancers aim for clear margins to prevent local recurrence. However, up to 20% of cases result in positive margins, with secondary surgery increasing the chances of death after 5 years. We envision a MMF endoscope that collects high resolution images using wavefront shaping to scan a 405 nm beam at the fiber tip and collecting fluorescence intensity and lifetime to map tumor margins and detect residual malignant cells. To address the question whether the information contained in the fluorescence and morphology can be used to classify cancer and normal tissues, we used images acquired with a microscope and artificial neural network. Initial findings show promise to separate cancer from normal tissue when training neural networks on FLIM data. Spatial and temporal resolution and required field of view for effective margin assessment are determined.

1 Introduction

Head and neck cancers account for nearly a million diagnoses worldwide each year. Surgery is plagued by the frequent incidence of local tumor regrowth following surgery alone or in combination with adjuvant therapy. This incidence is found to be as high as 20% and felt to be the consequence of an aggressive tumor biology with infiltrative growth patterns, due to the complex anatomy of the surgical site or linked to sampling errors. In any case the detection of a positive surgical margin during surgery would allow for an immediate correction of the resection and produce a complete tumor resection, thus reducing the incidence of detrimental local recurrences. . Therefore, there is a pressing need for a point-of-care method capable of accurately mapping tumor margins in three dimensions before resection, as well as detecting residual cancer cells in the wound bed during resection.

The tool we design is a needle-like endoscope based on a multimode fiber (MMF), which allows for deep imaging and diffraction-limited resolution using the transmission matrix method [1,2]. The contrast mechanism is based on endogenous fluorescence of the cells. Tumor cells have a different metabolism than healthy cells, which affects their fluorescent lifetime response [3].

This presentation shows that lifetime can be used as the contrast mechanism to differentiate cancerous from normal tissue. The requirements in terms of excitation power, resolution (spatial and temporal), and field of view (FOV) needed to collect images with enough relevant information to implement a machine learning algorithm to classify tissue as cancerous or normal are defined in order to design the endoscope accordingly.

2 Material and methods

The images are collected using a Leica SP8 FLIM microscope. This microscope allows FLIM measurements with a pulsed 440 nm laser with 40 MHz repetition rate. Excitation at 405 nm is more efficient to reveal interesting metabolic behaviors [4]. Thus, we compare the intensity in the image between excitation at 440 nm and 405 nm, with 0.47 mW impinging on the sample, and derive an empirical factor. Following Hassan et al. work [5], lifetime images were collected in two emission bands, adapted to fit the laser excitation of 440 nm, namely CH2 corresponding to 473 ±13 and CH3 corresponding to 542 ± 25 nm. These channels correspond to the emission maxima of NAD(P)H and FAD and respectively. The dwell time is set to 1.2µs, and the resolution as 1 µm (the immersion objective has an NA of 0.95).

The samples are sagittal sections of a cryopreserved primary tumor and recurrent tumor attached to the floor of the mouth of mice injected into the submental space with the tumor cell line mEERL95 (ref.: PMID: 29313973).

H&E stains of a subsequent layer from each sample are used to define the labels. 22 images of and 107 images of normal tissue are collected for training and 30 images of margin are kept to test the segmentation overlay. The network inputs contain 3 channels corresponding to the lifetimes in CH2 and CH3 and the intensity ratio. The original full-sized images (512x512 pixels) are cropped

* Corresponding author: victoria.fay@epfl.ch

into smaller images. Due to an imbalance in the ratio of normal and cancerous images, we augment the cancer class by rotations, resulting in 6592 images in the normal class and 5376 images in the cancer class. The model is a U-net with 5 layers and 1862849 trainable parameters. It is trained on down-sampled inputs to identify the spatial resolution, time resolution and FOV at which the classification/segmentation fails.

The first version of the endoscope setup allows for FD-FLIM measurements at 405 nm through a MMF, using an internally modulated laser diode. At the distal side, a 3-axis stage allows to bring the sample to the tip of the fiber. A dichroic mirror allows separation of the excitation light and transmitted fluorescence from the proximal end of the fiber. The fluorescence is detected and compared to a reference to determine the lifetime.

3 Results

It was determined that the fluorescence intensity excited at 405 nm is about 3 times larger than when excited at 440nm. Fig. 1 shows the model performs better on a larger FOV, however, the difference in accuracy is minimal and the accuracies equalize when training the smaller FOV on a larger number of samples. The accuracy drops as spatial resolution decreases. below 4 µm, the convergence slows down. High temporal accuracy such as picoseconds is not required, as the accuracy remains stable until a resolution of 6 ns. To verify that lifetime measurements do play a role in the classification and that the consistency despite down sampling isn't due to the sole spatial information from the intensity ratio, accuracies are compared for training using only the intensity ratio channel or all available lifetime information. Adding lifetime information increases the accuracy from 80 to 90%.

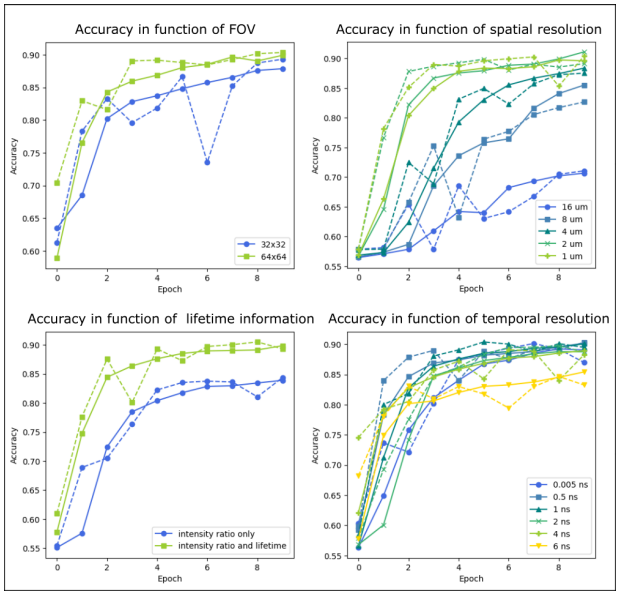

Fig. 1. Classification accuracy in function of imaging parameters (FOV in pixels, lifetime, spatial and temporal resolutions in µm and ns respectively).

Fig. 2 shows that cancer near the margin is properly classified, even in an island within normal tissue. There are some false positives, however no false negatives were observed in this sample.

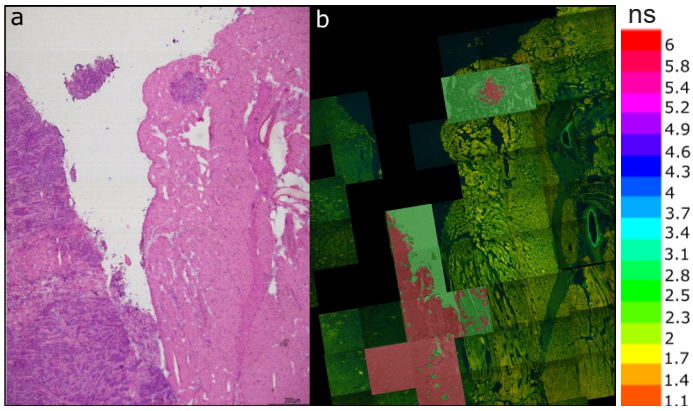

Fig. 2. a: H&E stain of the sample. b: false colored FLIM images collected on the Leica microscope in CH3, brightness represents fluorescence intensity and hue represents lifetime. Predictions are overlaid on the margin areas in green and red corresponding to normal and cancer classes respectively.

4 Conclusions

Freedom in spatial resolution allows some play in the diameter of the fiber core as well as focusing method and can improve the real-time factor of the measurement. The minimal required temporal accuracy is of the order of 4 ns which should be reached even with noisy detection. Finally, the field of view provided by thin fibers contains enough information for classification, allowing segmentation at each shot, rather than after a cumulation of them.

Funding: This work was supported by the TANDEM grant from the ISREC Foundation. The authors would like to acknowledge Severine Urfer for her invaluable assistance in preparing the samples. Her expertise and dedication were instrumental in the execution of this research.

References

1. A. Boniface, J. Dong, S. Gigan, Nat Commun 11 (2020)
2. D. Loterie, S. Farahi, I. Papadopoulos, A. Goy, D. Psaltis, C. Moser, Opt. Express **23** (2015)
3. R. Datta, T.M. Heaster, J.T. Sharick, A.A. Gillette, M.C. Skala, J. Biomed. Opt. **25**, 7 (2020)
4. J. Deal, S. Mayes, C. Browning, S. Hill, P. Rider, C. Boudreaux, T.C. Rich, S.J. Leavesley, J. Biomed. Opt. **24,** 2 2019
5. M.A. Hassan, B.W. Weyers, J. Bec, F. Fereidouni, J. Qi, D. Gui, A.F. Bewley, M. Abouyared, D.G. Farwell, A.C. Birkeland, L. Marcu, IEEE T. Biomed. Eng. **70**, 10 (2023)